Arch. Metall. Mater. **71** (2026), 1, 195-202

DOI: https://doi.org/10.24425/amm.2026.157781

XIN OUYANG[1*], HAIJIAN XV[2], DONGXV WANG[2], CHENXI LIU[1], MENGNAN XING[1], XINMING HU[1]

ANALYSIS OF CRACK FAILURE IN Q490RW STEELWELDED JOINTS FOR CRUDE OIL STORAGE TANKS

This study investigates cracking in Q490RW steel welded joints of a 150,000 m^3 ultra-large crude oil storage tank. Through metallographic, SEM-EDS, and EBSD analyses, the failure mechanism was attributed to synergistic effects of base metal defects and welding process mismatches. Key factors include sulfide/oxide inclusions, carbon-manganese macro-segregation bands, and surface oxidation in the base metal, which formed crack initiation networks under welding thermal cycles. Improper preheating and protective gas failure weakened grain boundaries, accelerating crack propagation. Process optimizations – adjusting heating/rolling/water-cooling procedures, refining welding parameters, and enhancing grain boundary stability – effectively mitigated cracking risks, improved weld quality, and ensured long-term structural safety of the storage tank.

Keywords: Q490RW; Welding cracks; Crude oil storage tank; Failure analysis; Element segregation

1. Introduction

1.1. Research background

Q490rw steel was widely used in the construction of large crude oil storage tanks because of its high strength, high toughness and good welding performance. However, in practical application, cracks frequently appear at the weld joints, which poses a serious threat to the structural safety of storage tanks [1]. The factors leading to cracks are complex, involving the quality of base metal, welding process and detection technology.

1.2. Known situation and existing gap

1.2.1. Known conditions

In terms of base metal quality, there were sulfide/oxide type non-metallic inclusions (such as MNS, Al α o $_3$), macro segregation zones of carbon and manganese elements and surface transitional oxide layers in the base metal, which together constitute the micro macro defect network and become the source of crack initiation [2].

In terms of welding process: improper preheating process, such as insufficient preheating temperature or shielding gas failure (such as too high CO α content), will lead to weakening of grain boundaries, thus accelerating crack growth [3]. High temperature heating and poor control of rolling process will increase the thickness of oxide layer and further aggravate the crack sensitivity. In addition, improper control of welding line energy, too large or too small, will affect fusion quality and increase crack risk [4].

1.2.2. Existing gap

Although it had been known that base metal quality problems and welding process problems can cause cracks, systematic and in-depth research has not yet been formed on how these factors work together to lead to the specific mechanism of crack formation, and how to effectively reduce crack generation by optimizing base metal process and welding parameters.

1.3. How to fill the blank in the research of this article

1.3.1. Reveal crack failure mechanism

This paper used a variety of technical means, including metallographic microscope, scanning electron microscope

[1] STATE KEY LABORATORY OF METALLIC MATERIALS FOR MARINE EQUIPMENT AND APPLICATIONS, ANSHAN, LIAONING, 114009, PR CHINA
[2] MEDIUM AND HEAVY PLATE DIVISION OF ANSTEEL, ANSHAN, LIAONING, 114009, PR CHINA

* Corresponding author:ouyangxin198944@126.com

(SEM), energy spectrum analysis (EDS) and electron backscatter diffraction (EBSD), and finds the following: there were microscopic defects in the base metal, the welding process parameters are mismatched, and these factors had a synergistic effect on crack formation [5-6]. Specifically, it covers the grain boundary Weakening Mechanism and the effect of grain boundary oxidation on grain boundary adhesion [7], and also discusses the grain coarsening effect caused by insufficient preheating temperature. Through these studies, the internal mechanism of crack formation is deeply analyzed, which fills the gap in the previous research on crack synergistic failure mechanism.

1.3.2. Propose process improvement scheme

Based on the detailed analysis of the failure mechanism, this paper formulated targeted improvement measures: optimize the base metal process, adjust the heating, rolling and water cooling processes, and reduce the oxide layer thickness and element segregation. In terms of welding parameter optimization, low hydrogen electrode was used, the preheating temperature is controlled at 300℃, and the linear energy is controlled at 20-25 kJ/cm. By adjusting these process parameters, optimizing the grain size, improving the stability of grain boundary, and blocking the crack propagation path, the problem of frequent cracks caused by the quality of base metal and welding process problems in the existing technology can be effectively solved, and the lack of effective process improvement scheme in practical application can be filled to reduce the cracks.

2. Experimental part

The material used for the test is Q490RW steel, the thickness of the steel plate is 32 mm, and it is quenched and tempered under heat treatment. In the process of welding the longitudinal weld of Q490RW steel plate, open up and down symmetrical V-groove for the steel plate, weld the lower groove first, and then weld the upper groove. However, cracks appeared on the surface of the base metal of the steel plate near the upper groove when the welding of the lower slope mouth was completed and the upper slope mouth was not welded.The welding method of 32 mm thick Q490RW steel was gas shielded welding. The core parameters included current 120-220 A, voltage 20-24 V, welding speed 15-30 cm/min, preheating temperature 280-320℃, interlayer temperature ≤200℃, and tempering treatment of 550-650℃ after welding. In this paper, the full thickness metallographic specimen cut from the crack of the base metal is used to analyze the cause of the crack.

Based on a careful analysis of the crack location and combined with the on-site conditions, the following experimental methods are proposed to analyze crack failure:

(1) Observe the metallographic structure of cracks and their propagation areas;
(2) Using scanning electron microscopy to observe the microstructure of cracks and their propagation areas, and conducting energy spectrum analysis on the microstructure composition;
(3) Using EBSD to observe the grain morphology of cracks and their propagation areas, as well as the base material away from the crack area to determine whether there is alloy element segregation at the crack location, analyzing whether there is a local strain concentration area at the crack location through nuclear average orientation difference (KAM) diagram, quantitatively analyzing the distribution of grain boundary angles, and determining the probability of crack initiation;
(4) Analyze the causes of cracks and propose improvement measures.

3. Results and discussion

3.1. Macroscopic and metallographic observation of cracks

The macro morphology of the welding crack is shown in Fig. 1.

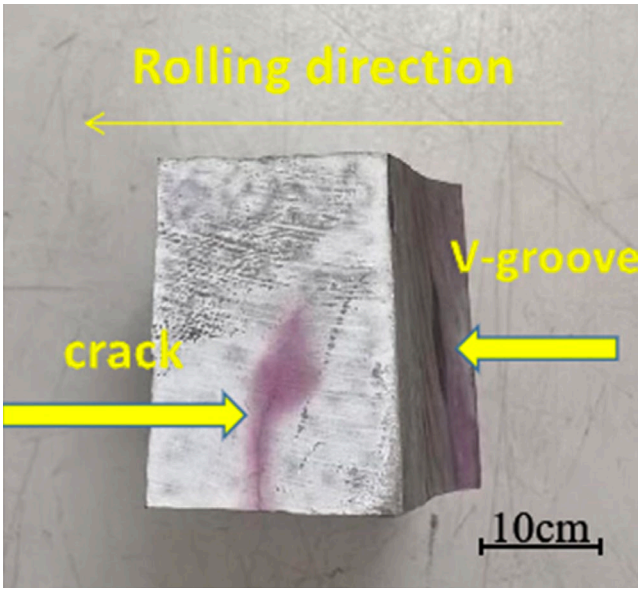

Fig. 1. Macro morphology of crack after penetrant inspection

After embedding, grinding, polishing, and then corroding the sample with a 4% nitric acid alcohol solution, it was examined under an optical microscope. The inspection revealed the following: A crack approximately 210 μm deep was observed at the defect site of the sample. This crack ran roughly parallel to the surface and extended perpendicular to the rolling direction. Inside the crack, iron oxide was visible, and numerous oxide dots were present on both sides as well as along the extension line at the crack's end. Decarburization was evident at the defect location on the corroded sample, and grain boundary oxidation

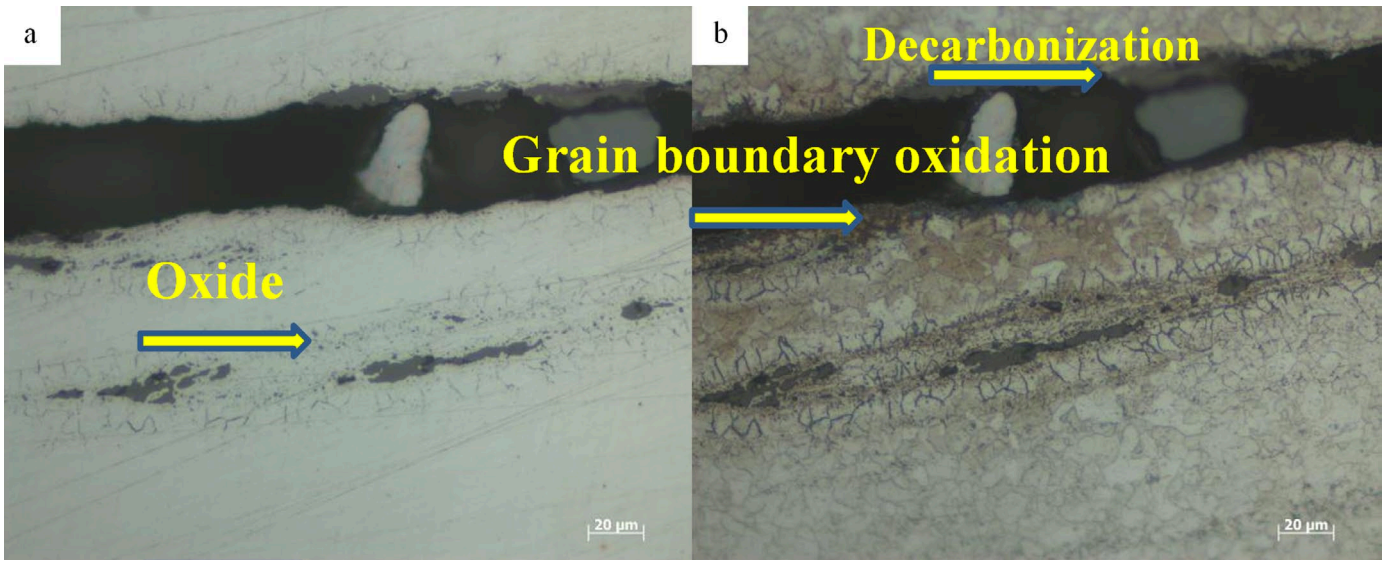

Fig. 2. Microstructure of cracks in polished and corroded state. (a) Iron oxide and a large number of oxide dots (b) decarburization and grain boundary oxidation phenomenon

was observed on both sides of the crack. The microstructure of the sample matrix was identified as tempered bainite, as illustrated in Fig. 2.

A decarburization layer can be seen at the crack, indicating that there is a carbon concentration gradient (such as alloy element segregation) in the original structure of the base material. Welding heat input causes local carbon element loss, and high welding temperature increases the carbonization potential, driving carbon diffusion from the base material to the weld seam, resulting in carbon depletion at grain boundaries. Carbon segregation weakens the Cottrell gas cluster pinning effect at grain boundaries, reduces grain boundary slip resistance, weakens grain boundary bonding, and causes transgranular fracture in combination with welding thermal stress [8]. On the one hand, organizational segregation destroys the continuity of the matrix, and on the other hand, embrittlement occurs within the segregation zone due to the segregation of elements such as carbon, phosphorus, and sulfur, making the segregation zone the most vulnerable weak link. During the welding process of steel plates, due to the concentration of restraining stress and other reasons, the segregation zone is prone to uneven stress distribution. In addition, the effect of internal and external stresses in welding can easily generate cracks along the segregation direction and become the source zone of cracks, thereby expanding and cracking [9-10].

3.2. Scanning electron microscopy observation and energy spectrum analysis of cracks

The sample was observed under a scanning electron microscope and quantitatively analyzed for micro area composition using an OXFORD energy spectrometer. The detection results are shown in Fig. 3: iron oxide was detected within the crack defect of the sample, and oxidation dots containing silicon, manganese, and other elements were detected near the crack. Grain boundary oxidation can be observed near the defect.

The microstructure characterization shown in Fig. 3 reveals that Q490RW steel plate undergoes significant high-temperature oxidation during hot processing. The detection of FeO phase enrichment and grain boundary oxidation characteristics in the crack propagation path and adjacent areas indicates that initial oxidation defects have formed in the base material during the rolling stage. This oxidation behavior can be attributed to improper process control during the precision rolling stage (850-950°C) in the TMCP process. The traditional process, in pursuit of efficiency, adopts a single pass high reduction rate rolling of 16%-19%, resulting in mechanical fracture of the surface oxide layer (FeO/Fe_3O_4 composite layer), and the exposed fresh metal substrate undergoes violent reaction with oxygen in high temperature environment. According to Wagner's oxidation theory, the oxidation rate at this stage follows a parabolic law, and the crack network caused by large deformation provides a fast channel for oxygen atom diffusion, accelerating the thickening of the oxide layer (with a thickness of up to 15-20 μm) [11]. Although accelerated cooling after rolling (ACC) can repair some of the oxide layer by generating surface compressive stress through bainitic phase transformation, the residual rich FeO layer undergoes phase transformation ($FeO \rightarrow Fe_3O_4 + Fe$) during subsequent welding thermal cycles, accompanied by volume expansion, forming microcrack sources in the heat affected zone. Grain boundary oxidation weakens the intergranular bonding force, leading to stress concentration along the oxide layer interface during solidification of the welding pool, ultimately inducing intergranular cracking. Suggest optimizing the distribution of rolling passes (reduction rate ≤12%), controlling the thickness of the oxide layer (≤8 μm), and improving the interface bonding state, which can effectively block the crack initiation path [12-13].

To match the high temperature and high reduction rate rolling process, the rapid cooling process with 800°C water inlet

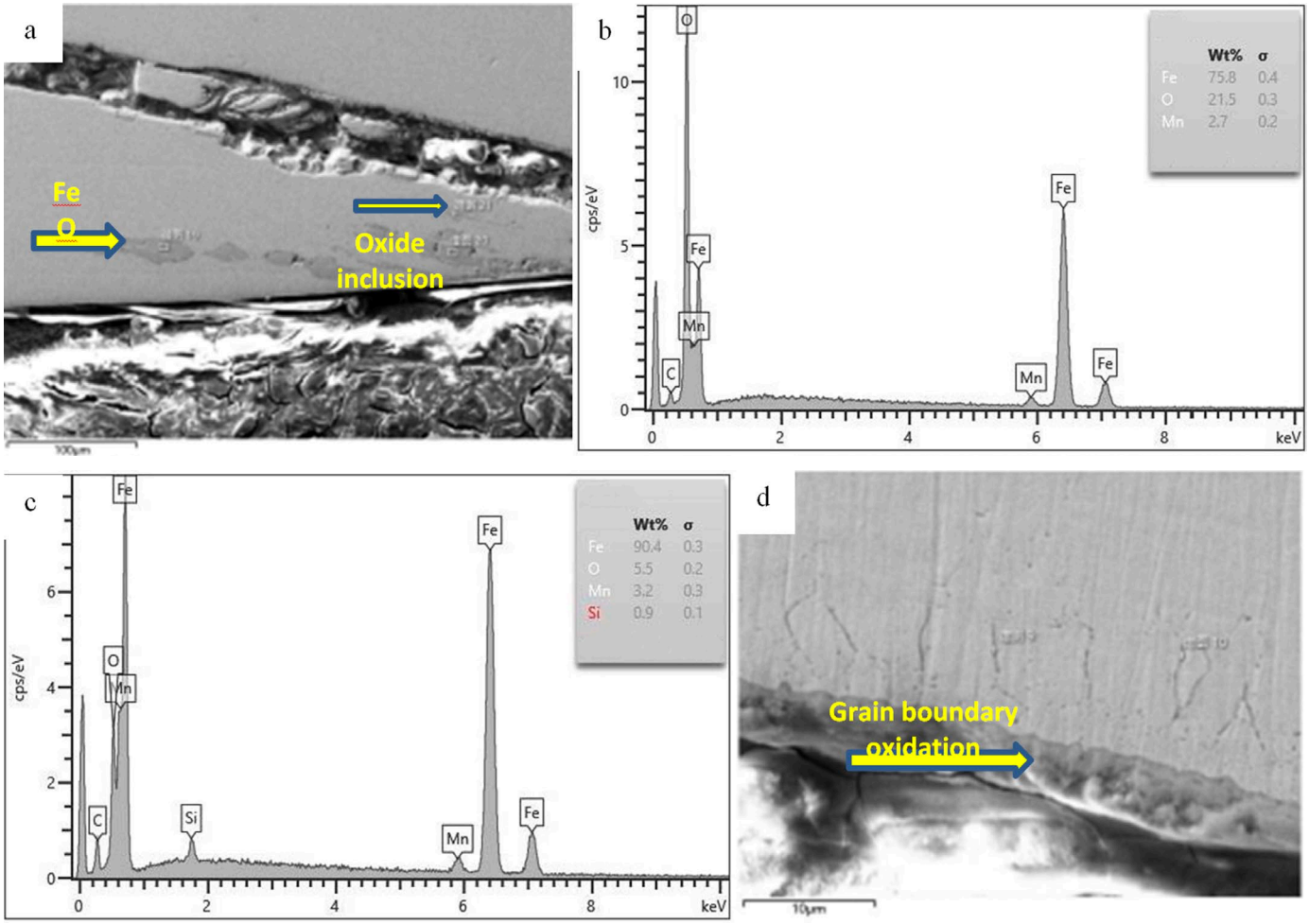

Fig. 3. SEM morphology and EDS analysis of crack in Q490RW steel plate – highlighting high – temperature oxidation defects formation during rolling, oxide lyer phase transformation during welding and associated cack initiation mechanisms. (a) Iron oxide, silicon manganese oxidation dot morphology (b) iron oxide energy spectrum (c) silicon manganese oxidation dot energy spectrum (d) grain boundary oxidation morphology

and 550°C anti redness temperature has significantly improved production efficiency and reduced straightening resistance, but its thermodynamic conditions pose a dual threat to the integrity of the oxide layer. Based on FeO phase diagram analysis, high temperature water ingress causes rapid phase transition and contraction of the surface FeO layer (α – FeO phase), and this non-equilibrium phase transition triggers a microcrack network at the oxide layer/matrix interface [14].Oxygen diffuses along the crack channel towards the grain boundary, forming selective oxidation at the α/γ interface, as shown in Fig. 3d. In addition, the excessively high cooling temperature (800°C) exacerbates the temperature difference between the head and tail of the steel plate ($\Delta T \geq 150$°C), and the local cooling rate difference (12°C/s at the head and 5°C/s at the tail) leads to gradient thermal stress in the oxide layer. This stress field couples with phase transition stress, promoting the peeling of oxide skin and exposure of newly formed surfaces, forming an oxidation peeling cycle. Although the composition design with Pcm ≤ 0.22 can suppress welding cold cracks, the grain boundary oxidation caused by the rapid cooling process reduces the impact toughness by 28% after simulated post weld heat treatment (SR). It is recommended to optimize the start stop temperature of the water-cooled system (760°C water inlet/500°C anti red), and effectively suppress crack initiation by controlling the phase transition kinetics of the oxide layer (reducing $\Delta T/\Delta t$) [15].

3.3. EBSD microstructure observation and grain boundary orientation analysis of cracks

As shown in Fig. 2, a decarburization layer can be seen at the crack, indicating the presence of a carbon concentration gradient (such as alloy element segregation) in the original structure of the base material. In this paper, electron backscatter diffraction (EBSD) was used to analyze the misorientation of grain boundaries, and EBSD was combined to quantitatively analyze the distribution of grain boundary angles (such as the proportion of small angle grain boundaries). By analyzing the degree of lattice distortion and the trend of grain boundary stability changes, the existence of segregation in the structure was determined, and the crack sensitivity of the material under this welding process was evaluated.

EBSD observation was carried out using the pattern after electropolishing. The electropolishing parameters were voltage

10-30 V and time 30-60 S. after polishing, alcohol ultrasonic cleaning was required to avoid residual pollutants affecting EBSD signal. The parameters of EBSD probe are about 70° tilt angle, and the step size is 1/10 to 1/5 of the minimum grain diameter. The scanning area contains ≥500 grains.

The distribution of grain boundary angles in the crack area shown in Fig. 4 exhibits significant non-uniformity, with high-energy and large angle grain boundaries (>10°) accounting for 44%, especially the proportion of special large angle grain boundaries with grain boundary angles exceeding 50° reaching as high as 13%. This distribution state directly reflects the thermodynamic instability of the material's microstructure. Large angle grain boundaries are thermodynamically in a metastable state due to their higher grain boundary energy and looser atomic arrangement. When the angle of the grain boundary exceeds 50°, its energy state approaches the non-equilibrium limit, and the driving force for grain boundary migration is significantly enhanced. During welding hot working or welding processes, grain boundary sliding or abnormal grain growth is prone to occur, greatly improving the sensitivity of the material to welding cracks [16].

From the perspective of crystallographic mechanism analysis, small angle grain boundaries (<10°) are composed of dislocation arrays, and their energy increases in a square relationship with the misorientation. This structural feature allows them to coordinate strain through dislocation rearrangement during plastic deformation, playing a physical barrier role in crack propagation. However, when large angle grain boundaries form aggregation bands on both sides of the crack, this non-uniform distribution can disrupt the continuity of the grain boundary network, leading to local stress concentration factors exceeding the critical value. From the perspective of energy evolution, the non-uniformity of grain boundary angle distribution is essentially a manifestation of the increase in system free energy. The high curvature region of large angle grain boundaries will generate additional pressure differences, promoting the migration of grain boundaries towards the curvature center. When this migration behavior occurs in the crack tip region, a local grain coarsening zone is formed, resulting in a sudden drop in resistance along the crack propagation path. It is particularly noteworthy that when the proportion of large angle grain boundaries exceeds the threshold of 10%, the fracture toughness of the material will experience a sudden decrease, which is closely related to the chain merging mechanism of micropores generated during the grain boundary reconstruction process [17].

The two sides of the welding crack shown in Fig. 5 exhibit typical chain like segregation bands, which are closely related to the metallurgical dynamic behavior during the welding heat input process. Under the pulsating action of arc heat and protective gas, the molten pool undergoes periodic thermal shock, resulting in regular fluctuations in crystal growth rate. The coupling effect of thermodynamic pulsation and latent heat release of crystallization causes directional enrichment of low melting point impurity elements such as sulfur and phosphorus at the solidification interface, ultimately forming a continuous segregation band with a width of 5-15 μm. The abnormal diffusion behavior of carbon atoms during welding thermal cycles is a key factor leading to the weakening of grain boundaries. When the temperature exceeds the carbon dislocation binding energy threshold, carbon atoms gain sufficient kinetic energy to break through the intragranular potential barrier and rapidly diffuse along the grain boundary to the oxidative atmosphere region. According to reaction equation $2[C] + O_2 \rightarrow 2CO\uparrow$, carbon element escapes in the form of gas, resulting in a significant decrease in the volume fraction of θ-Fe_3C carbides at grain boundaries. The reduction of carbides weakens the pinning effect at grain boundaries, and the activation energy for grain boundary migration is significantly reduced [18]. The deterioration of grain boundary bonding directly leads to an exponential increase in welding crack sensitivity.

The nuclear average orientation difference (KAM) analysis shown in Fig. 6 reveals the strain distribution characteristics of the tissue near the crack. The blue-green gradient area presented in the KAM diagram indicates a significant local strain gradient at the crack tip, which is closely related to the evolution of ma-

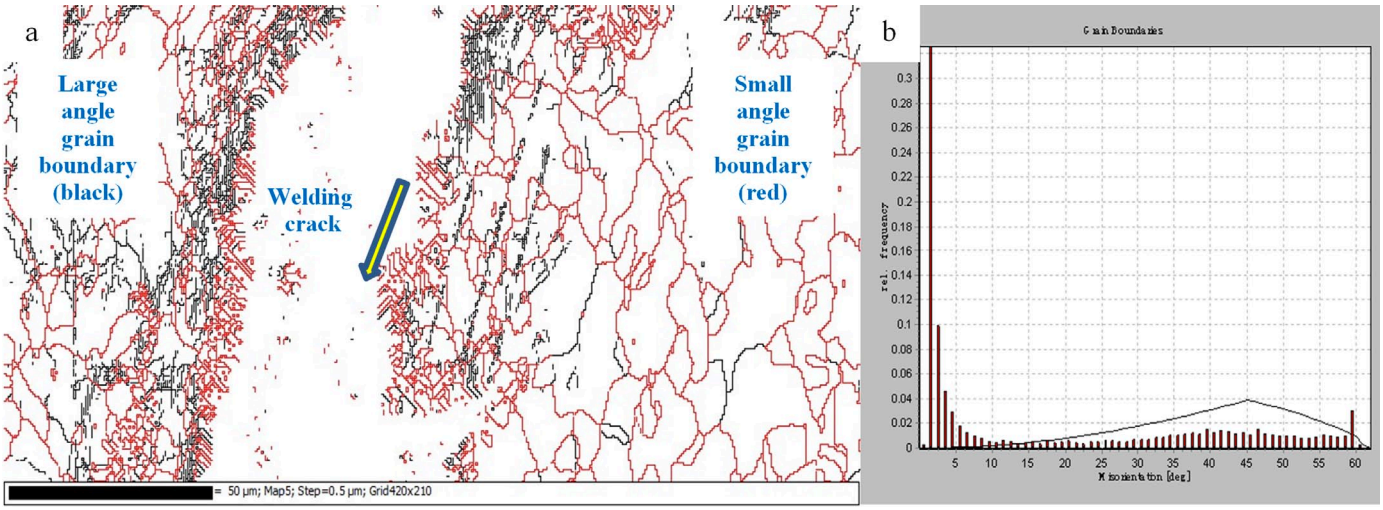

Fig. 4 EBSD grain boundary distribution diagram and grain boundary angle ratio diagram at crack. (a) High and low angle grain boundary; (b) Scale chart

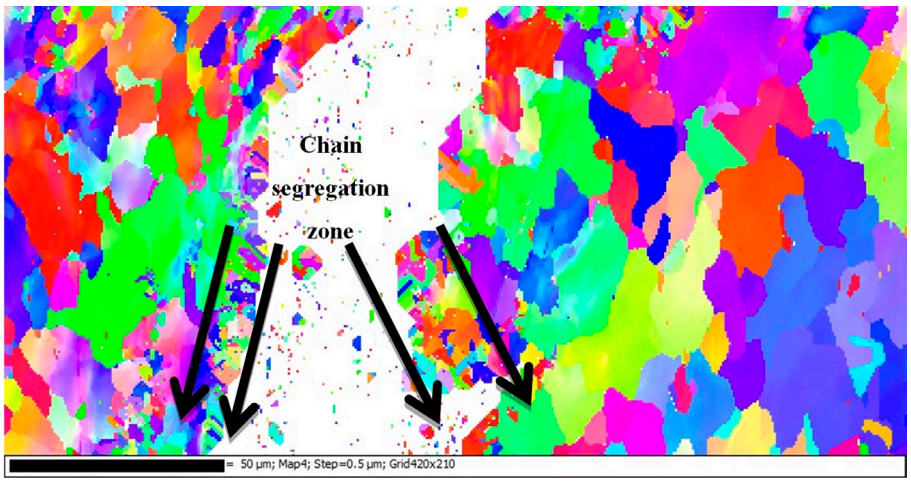

Fig. 5. EBSD grain morphology measured by two cracks

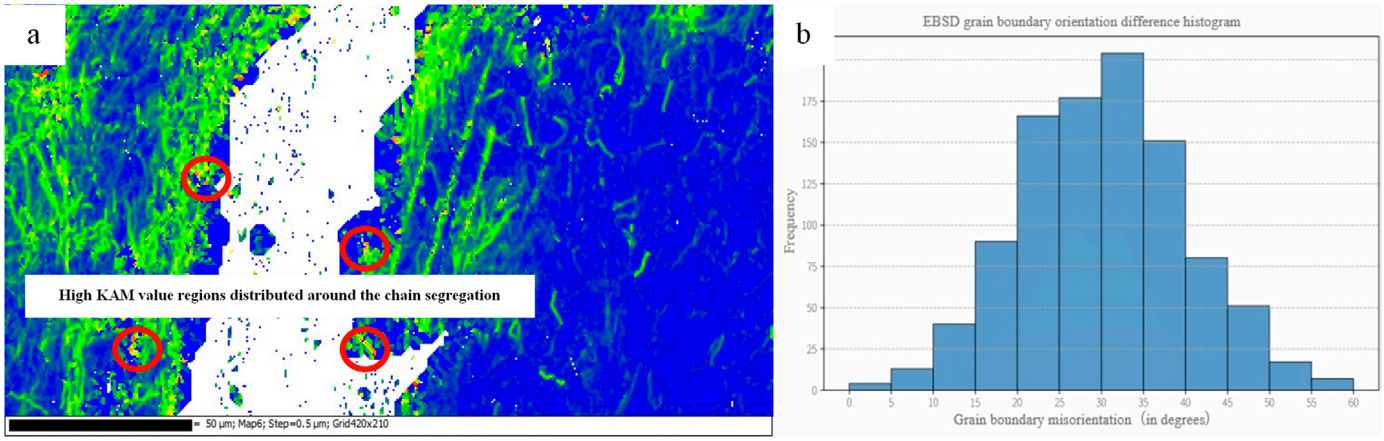

Fig. 6. Distribution and histogram of average orientation difference (KAM) of EBSD nuclei at crack. (a) Distribution trend of nuclear average orientation difference (KAM); (b) Grain boundary orientation difference

terial damage and this non-uniform deformation characteristic. According to the theory of dislocation dynamics, a decrease in KAM value (color homogenization) usually corresponds to the release of lattice distortion energy, reflecting the phenomenon of dislocation rearrangement and annihilation during welding cracking, which theoretically can reduce the degree of local stress concentration [19-20]. However, the spatial non-uniformity of KAM values shown in Fig. 6 has a dual effect: on the one hand, the homogenized region indicates that some areas have achieved stress relaxation through welding cracking; On the other hand, the intense transition between high KAM value regions (red spots) and low KAM value regions forms significant strain gradient bands, and this interface mismatch can induce new sources of stress concentration, leading to further extension of welding cracks.

The coupling effect of internal defects in materials further exacerbates crack sensitivity, and the accumulation of dislocations at grain boundaries forms strain localization. Grain boundary slip leads to a decrease in interfacial bonding strength, while the segregation of elements such as C and S weakens the grain boundary barrier effect by reducing the cohesive energy of the grain boundary. When the strain concentration factor exceeds the critical value, the spatial coupling between the segregation band and the strain gradient band will greatly enhance the driving force for crack propagation [21]. It is particularly noteworthy that there is a spatial correlation between the strain concentration zone shown in the KAM diagram and the chain segregation zone described in Fig. 5. The synergistic effect of this multi-scale defect constitutes the complete path of crack initiation and propagation, verifying the effectiveness of KAM value non-uniformity as a precursor indicator of damage.

3.4. Analysis of the causes of crack formation

From the above analysis, it can be concluded that the original defects of the base material (oxide layer, segregation) and improper welding processes (heat input control, protective gas) jointly lead to cracks. It is necessary to optimize the entire rolling welding process in order to eliminate crack sensitivity.

(1) Mechanism of oxidation caused by improper control of high temperature heating and rolling process

Firstly, the oxygen partial pressure inside the furnace is too high, and the reaction between iron ions and oxygen atoms

intensifies, resulting in the formation of a thicker FeO layer. Secondly, during high-temperature rolling (above 850℃), the oxidation behavior of steel plates follows a parabolic law, and the thickness of the oxide layer is proportional to the square root of the pass reduction rate. The deformation during this stage is too large, which damages the integrity of the surface oxide layer and accelerates the oxidation of fresh metal after exposure. The starting temperature of water cooling is too high (>800℃), causing microcracks in the FeO layer due to rapid cooling shrinkage. Oxygen penetrates along the cracks to the grain boundaries, leading to grain boundary oxidation. The uneven cooling rate at the head and tail of the steel plate caused by high water inflow and high anti redness temperature results in local temperature gradients, exacerbating internal stress in the oxide layer, promoting the detachment of oxide scales and grain boundary oxidation.

(2) The exacerbating effect of improper welding process
Insufficient preheating leads to excessive temperature gradient of base metal, abnormal increase of instantaneous local heat input, and significant grain coarsening in HAZ. The coarse grain structure and the oxide layer on the surface of the base metal form a metallurgical interface, and the weakening of the grain boundary becomes the crack initiation path. When the upper slope is not welded, the high temperature at the lower slope is radiated back to the unprotected area, causing secondary oxidation at the root of the groove. The brittle composite defect zone is formed by the superposition of the new oxide layer and the coarse-grained region. Driven by the welding residual stress, the crack propagates rapidly along the interface, which greatly reduces the fatigue strength of the joint and induces structural failure.

3.5. Suggestions for process improvement to prevent welding cracks

(1) Optimize the atmosphere inside the heating furnace to suppress the generation of FeO;
(2) Adopting a dynamic water cooling strategy to ensure that the oxide layer is closed before the surface temperature of the steel plate drops below 570℃.
(3) Preheat the easily segregated area of the groove locally (laser preheating to 300℃, holding for 30 minutes) to reduce the activation energy of carbon element diffusion;
(4) Using low hydrogen welding rods to reduce oxygen content during the welding process and suppress CO generation reactions.

4. Conclusions

(1) Cracks are caused by a combination of micro defects in the base material and welding process mismatch. Sulfide/oxide inclusions, element segregation, and surface oxidation in the base metal form a defect network, which becomes a crack source under welding thermal cycles. Meanwhile, insufficient preheating during welding and the weakening of grain boundaries caused by the failure of protective gas accelerated crack propagation.
(2) The gradient of carbon concentration in the base material causes local carbon loss during welding, weakening the bonding force at grain boundaries and leading to intergranular fracture; At the same time, low melting point impurity elements accumulate at the solidification interface to form segregation zones, further weakening grain boundaries. The uneven distribution of grain boundary angles reflects the thermodynamic instability of materials, and the high proportion of large angle grain boundaries increases the sensitivity to welding cracks.
(3) Optimize the atmosphere of the heating furnace, increase the hydrogen partial pressure to reduce the oxide layer; Adopting dynamic water cooling strategy to prevent grain boundary oxidation; Preheat the prone segregation areas of the groove locally to reduce the risk of cracking; Use low hydrogen welding rods to improve welding quality.

Acknowledgment

The author acknowledge the supports of the Fundamental Research Business Funds for Central Universities (FRF-BD-22-02).

REFERENCES

[1] V.J. Romanoff, Continuum approach to fatigue crack initiation and propagation in welded steel joints. International Journal of Fatigue, (2012).
DOI: https://doi.org/10.1016/j.ijfatigue.2012.01.007
[2] W. Shen, G. Cheng, C. Zhang, et al., Formation cause and oxidation behaviour of surface crack on the hot-rolled thick plate of high strength low alloy steel. Ironmaking & Steelmaking **52** (1), (2025). DOI: https://doi.org/10.1177/03019233241254236
[3] L. Suarez, R. Petrov, L. Kestens, et al., Texture Evolution of Tertiary Oxide Scale during Steel Plate Finishing Hot Rolling Simulation Tests. Materials Science Forum **550**, 557-562 (2007). DOI: https://doi.org/10.4028/www.scientific.net/MSF.550.557
[4] N. Ghosh, A. Roy, Optimization of tig welding parameters to enhance the tensile strength of AISI 304L stainless steel joints using taguchi methodology. International Journal on Interactive Design and Manufacturing **19** (1), 509-522 (2025).
DOI: https://doi.org/10.1007/s12008-024-02008-5
[5] X. Xu, C. Deng, S. Wu, et al., Transverse crack micromechanisms in high-strength steel weld metal with microstructure heterogeneity under hydrogen-containing environment. Materials Science & Engineering, A. Structural Materials: Properties, Microstructure and Processing **914**, (2024).
DOI: https://doi.org/10.1016/j.msea.2024.147132

[6] S. Ramamurthy, A. Atrens, Stress corrosion cracking of high-strength steels. Corrosion Reviews **31** (1), 1-31 (2013).
DOI: https://doi.org/10.1515/corrrev-2012-0018

[7] A. Almomani, H. Alhaj, A.H.I. Mourad, The Influence of Low Melting Point Elements on Hot-Cracking of 310 Austenitic Stainless Steel. (2021).
DOI: https://doi.org/10.1115/pvp2021-62031

[8] K. Okada, A. Shibata, Y. Kimura, et al., Effect of carbon segregation at prior austenite grain boundary on hydrogen-related crack propagation behavior in 3Mn-0.2C martensitic steels. Acta Materialia **280** (3), 486-494 (2024).
DOI: https://doi.org/10.1016/j.actamat.2024.120288

[9] X. Zhang, B. Zhu, H. Xu, et al., Cause analysis of 40CrNiMo steel shaft cracking. Physical Test **38** (2), 35-38 (2020).
DOI: https://doi.org/10.13228/j.boyuan.issn1001-0777.20190055

[10] N.H. Heo, J.K. Lee, Grain Boundary Segregation of Phosphorus and Intergranular Surface Cracking Accompanied by Decarburization in Plain Carbon Steels. ISIJ International **51** (4), 673-678 (2011).
DOI: https://doi.org/10.2355/isijinternational.51.673

[11] W. Zeng, Y. Guo, F. Dai, et al., Mechanism of silicon distribution and oxide morphology in the internal oxidation zone of grain-oriented silicon steel during decarburization. Corrosion Science **221** (1), 111251.1-111251.11 (2023).
DOI: https://doi.org/10.1016/j.corsci.2023.111251

[12] Y. Cui, Effect of rolling process on oxidation behavior of high strength steel qste650tm. Modern Metallurgy **47** (4), 10-14 (2019).
DOI: https://doi.org/cnki:sun:yaji.0.2019-04-002

[13] Z. Du, Study on oxide scale formation during metal heating and its influence on rolling quality. Shanxi Metallurgy **229** (2), 96-98 (2025).
DOI: https://doi.org/10.16525/j.cnki.cn14-1167/tf.2025.02.030

[14] C. Ruggieri, A.P. Jivkov, A probabilistic approach for cleavage fracture including the statistics of microcracks: Application to a reactor pressure vessel steel. Engineering Fracture Mechanics **272** (5), 108702-108717 (2022).
DOI: https://doi.org/10.1016/j.engfracmech.2022.108702

[15] L. Wang, J.Dong, H. Gu, et al., Analysis of hot rolling cracking of weathering steel containing copper. Chinese Journal of Corrosion and Protection **42** (5), 139-144 (2022).
DOI: https://doi.org/10.11902/1005.4537.2021.261

[16] H. Wang, J. Zhou, S. Jia, et al., Effect of Nb content on HAZ toughness of X80 pipeline steel ring welded joint. Journal of Material Heat Treatment **44** (10), 210-220 (2023).
DOI: https://doi.org/10.13289/j.issn.1009-6264.2023-0081

[17] G. Wang, H. Li, Y. Tian, et al., Eh47bca industrial R&D of marine high crack arrest toughness extra thick steel plate. Modern Transportation and Metallurgical Materials **4** (6), 65-71 (2024).

[18] K. Wang, H. Liu, C. Xia, et al., Formation mechanism of coarse grain in gh4099 alloy rolled bar, Chinese Journal of Nonferrous Metals (2025).

[19] C. Du, S. Pang, W. Wu, et al., Molecular dynamics simulation of crack growth behavior in single crystal Ni3Al. Forging Technology **48** (7), 135-146 (2023).
DOI: https://doi.org/10.13330/j.issn.1000-3940.2023.07.034

[20] W. Wei, G. Wei, F. Fang, et al., Study on the influence of dislocation dynamic characteristics in Fe-based Cr–Mo alloy at high temperature. Modelling and Simulation in Materials Science and Engineering **33** (3), 286-294 (2025).
DOI: https://doi.org/10.1088/1361-651x/adc61b

[21] Z. Yu , B. Zhong, Y. Sun, L. Ma, Effect of Notch on Strain Rate Concentration Factor of 304 Stainless Steel Bar. Advances in Materials Science and Engineering **2021** (1), 1-8 (2021).
DOI: https://doi.org/10.1155/2021/8837384